Square-wave oscillations in a semiconductor ring laser subject to counter-directional delayed mutual feedback

Song-Sui Li[1,*], Xiao-Zhou Li[1], Jun-Ping Zhuang[1], Gabor Mezosi[2], Marc Sorel[2], and Sze-Chun Chan[1,3]

[1] *Department of Electronic Engineering, City University of Hong Kong, Hong Kong, China*
[2] *School of Engineering, University of Glasgow, Rankine Building, Glasgow G12 8LT, UK*
[3] *State Key Laboratory of Millimeter Waves, City University of Hong Kong, Hong Kong, China*
[*] *Corresponding author: songsui.li@my.cityu.edu.hk*

Square-wave (SW) switching of the lasing direction in a semiconductor ring laser (SRL) is investigated using counter-directional mutual feedback. The SRL is electrically biased to a regime that supports lasing in either counter clockwise (CCW) or clockwise (CW) direction. The CCW and CW modes are then counter-directionally coupled by optical feedback, where CCW-to-CW and CW-to-CCW feedback are delayed by τ_1 and τ_2, respectively. The mutual feedback invokes SW oscillations of the CCW and CW emission intensities with period $T \approx \tau_1 + \tau_2$. When $\tau_1 = \tau_2$, symmetric SWs with a duty cycle of 50% are obtained, where the switching time and the electrical linewidth of the SWs can be respectively reduced to 1.4 ns and 1.1 kHz by strengthening the feedback. When $\tau_1 \neq \tau_2$, asymmetric SWs are obtained with a tunable duty cycle of $\tau_1/(\tau_1 + \tau_2)$. High-order symmetric SWs with period $T = (\tau_1 + \tau_2)/n$ can also be observed for some integer n. Symmetric SWs of order n = 13 with period T = 10.3 ns are observed experimentally.

OCIS codes: *140.5960, 140.3560, 190.3100*

Semiconductor ring lasers (SRLs) exhibit unique dynamics due to interactions of the longitudinal modes in both counter-clockwise (CCW) and clockwise (CW) directions [1–5]. Depending on the bias current, a free-running SRL has different operating regimes including bidirectional, unidirectional, and unstable lasing [1]. The unidirectional regime is often associated with bistability in which the lasing direction can be switched upon externally injected optical perturbations [6]. Such a unidirectional bistability has been investigated for implementing all-optical flip-flops [7]. On one hand, the logical operations of SRLs have been utilized to demonstrate NAND and NOR logical gates and optical regenerators [8–11]. On the other hand, using perturbations based on delayed optical feedback, a SRL has been applied for generating square-wave (SW) dynamics, where the emission intensity of each direction periodically switches on and off [12].

SW optical signals are needed as clocks in signal processing and communication systems [13–23]. Utilizing external laser sources, SW generation has been investigated based on chromatic dispersion of mode-locked pulses, bistabilities in semiconductor optical amplifiers, and nonlinearities in opto-electronic oscillators [19–22]. SW generation has also been generated directly on the output signal of a laser source by polarization-switching in edge-emitting lasers [13–15] and in vertical-cavity surface emitting lasers [16–18].

Recently, SW generation was demonstrated using a SRL based on one-way cross-feedback, where the dominating mode was counter-directionally fed back to the laser after a delay τ [12]. From time $t = 0$ to τ, the SRL is not yet perturbed and so it emits in the dominating CCW direction. From $t = \tau$ to 2τ, light from the CCW emission is counter-directionally fed back into the SRL, causing the laser to switch to CW emission, which in turn suppresses the CCW emission due to gain competition. At $t = 2\tau$, there is no longer any feedback to maintain the CW emission, so the SRL returns to emitting in the CCW emission through relaxation. The SRL emission thus switches between CCW and CW directions with a periodicity $T = 2\tau$. However, this approach employed only a one-way CCW-to-CW feedback, where no CW-to-CCW feedback was used. So the CW-to-CCW switching was not directly induced by any feedback, but it was entirely triggered by noise, which could cause significant jitter in the timing of the CW-to-CCW switching [12]. Also, the SW duty cycle was fixed at 50% without any tunability because of the one-way feedback.

In this Letter, a SRL subject to mutual counter-directional feedback is investigated experimentally. The SRL is under both CCW-to-CW and CW-to-CCW feedback, which are delayed by τ_1 and τ_2, respectively. Such a mutual feedback results in a very regular and deterministic switching of the emission direction. The observed SWs are periodic in $T \approx \tau_1 + \tau_2$ and the intensities of the two directions are complementary, with a tunable duty cycle of $\tau_1/(\tau_1 + \tau_2)$ for the CCW emission.

Figure 1(a) shows the experimental setup for realizing counter-directional mutual feedback into the SRL. The SRL is fabricated on an InP-based multi-quantum well (MQW) structure for lasing at around 1.57 μm and consists of a ring waveguide with a circumference of approximately 2.1 mm, which supports longitudinal modes with a free-spectral range of 40 GHz.

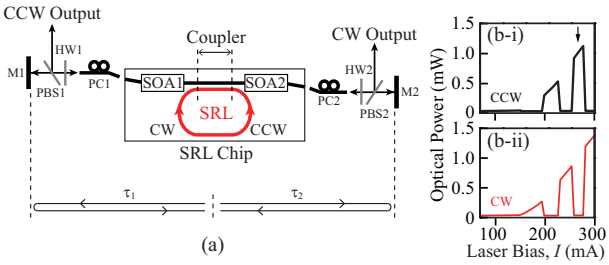

Fig. 1. (a) Schematic of a SRL under counter-directional mutual feedback. SRL, semiconductor ring laser; SOA, semiconductor optical amplifier; PC, polarization controller; HW, half-wave plate; PBS, polarizing beamsplitter; M, mirror. (b) Free-running optical power from the SRL chip versus the bias current for the CCW and CW emissions.

Through a directional coupler of 50% efficiency, the SRL is coupled to an output waveguide with a total length of 1 mm. The output waveguide has two independently biased sections that act as semiconductor optical amplifiers (SOAs) on both sides of the SRL. The waveguide intersects the cleaved facets of the chip at an angle of 12° to minimise back reflections into the laser cavity. The chip is temperature-stabilized at 16°C.

In order to implement CCW-to-CW feedback, the CCW emission from the SRL is first amplified by SOA1, collected by a lensed fiber with a polarization controller PC1 along with a collimator, and split through a half-wave plate HW1 by a polarizing beamsplitter PBS1. Half of the beam is reflected and used for monitoring the CCW output, while the other half is transmitted to a mirror M1. The reflected signal from M1 then passes again through PBS1, PC1 and SOA1, and couples back into the SRL in the CW direction. The CCW output in Fig. 1(a) is sent to a 43-GHz photodetector (Newport AD-10ir), where the instantaneous optical intensity is monitored by a real-time oscilloscope (Agilent 90254A) and the power spectrum is recorded by a spectrum analyzer (Agilent N9010A). The feedback round-trip delay time τ_1 is determined by the length of the free-space optics and the fiber on the left of the SRL. An identical arrangement is used on the right side of the chip for the CW-to-CCW feedback.

On each side, the polarization of the reflected beams from the mirrors into the SRL is kept aligned to that of the waveguide by adjusting the polarization controllers. The coupling efficiency from the waveguide to each lensed fiber is about 30% and the overall reflection as measured at the fiber input is about 18%. Biasing the SOAs from 0 to 30 mA yields a net single-pass gain from −6 dB to 1.5 dB. As a result, the coupling efficiency η between the counterpropagating modes can be adjusted from −36 dB to −21 dB. The bias currents of both SOAs are set equal to maintain the same efficiency for the CCW-to-CW and CW-to-CCW coupling.

With the SOAs floating electrically, the CCW (black) and CW (red) optical powers are recorded as the bias current I increases in Figs. 1(b-i) and 1(b-ii), respectively. From the threshold of 148 mA up to 155 mA, the SRL emits bidirectionally. Further increment of the bias current drives the SRL into unidirectional lasing operation in which the output emission switches between the CCW and CW mode as shown in Fig. 1(b). The bias is kept at I = 260 mA in the following measurements, where the SRL emits in the dominating CCW direction prior to the application of feedback as indicated by the arrow in Fig. 1(b-i).

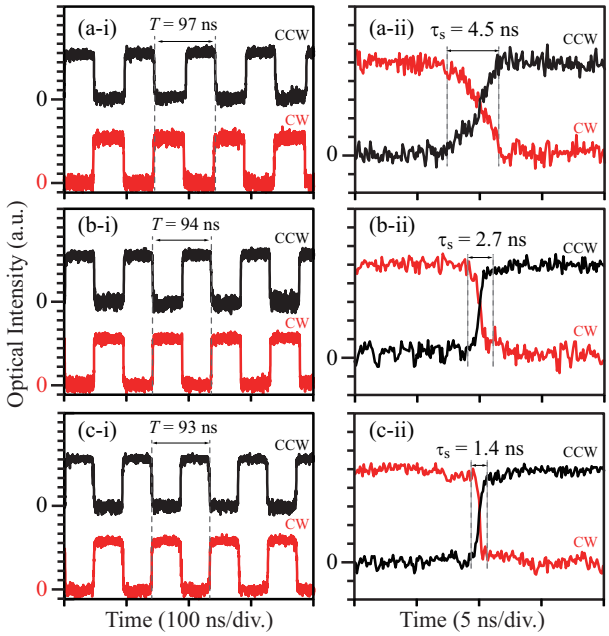

Fig. 2. Intensity-time traces of the SRL subject to feedback with $\tau_1 = \tau_2 = 45$ ns. The feedback efficiency is (a) $\eta = -36$ dB, (b) $\eta = -31$ dB, and (c) $\eta = -27$ dB. The two columns have different time spans to show the signal periodicity (left) and the SRL switching time (right).

With the counter-directional mutual feedback in Fig. 1, the SRL emits light in the CCW direction for a duration of τ_1 until light is fed back through the left side of the chip, thereby switching the SRL to emit in the CW direction. The CW emission continues for a duration of τ_2 until light is fed back through the right side of the chip, which switches the SRL back to CCW emission. As a result, the mutual feedback causes the SRL to emit CCW and CW intensities that exhibit SW oscillations. Figure 2 shows the intensity-time traces for the CCW (black) and CW (red) outputs under equal feedback delays of $\tau_1 = \tau_2 = 45$ ns, denoted by τ in the following text. The time traces are shown for increasing η from −36 dB to −27 dB in Figs. 2(a)–2(c), where the amplitudes of the SWs are normalized for comparison. The traces in column (i) are displayed over several SW cycles, where the traces for the CCW mode are up-shifted for visual clarity. Column (ii) is zoomed on the transient when the SRL emission switches from CW to CCW emission. The SWs of the two directions are complementary to each other and symmetrical as the duty cycle is 50%. The period T is slightly greater than 2τ due to the time needed for the directional switching in the SRL, though the difference diminishes as η increases. For instance, T reduces from 97 ns to 93 ns when η increases from −36 dB to −27 dB, as shown in Figs. 2(a-i)–2(c-i). The details of the transient when the SRL switches direction are shown in Figs. 2(a-ii)–2(c-ii). The switching time τ_s is quantitatively defined here as the duration taken by the output intensity to increase from 10 % to 90 % of its final value. When η increases from −36 dB to −27 dB in Figs. 2(a-ii)–2(c-ii), the switching time τ_s reduces from 4.5 ns down to 1.4 ns. Additionally, reducing η to below the minimum of −36 dB leads to a degradation of the SWs, where individual cycles are occasionally missing in the waveform. Such irregular waveforms have also been observed in another feedback configuration at

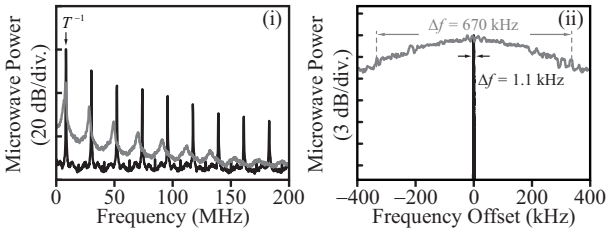

Fig. 3. Power spectra of the SRL subject to feedback with $\tau_1 = \tau_2 = 45$ ns plotted in (i) the baseband and (ii) a zoomed frequency span centered at T^{-1}. The feedback efficiency is $\eta = -36$ dB (grey) and -27 dB (black).

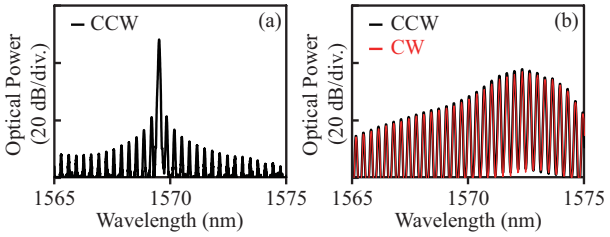

Fig. 4. Optical spectra of the SRL subject to (a) no feedback and (b) feedback of efficiency $\eta = -27$ dB. The CCW and CW spectra are shown in black and red, respectively. Resolution bandwidth: 0.06 nm.

low feedback efficiencies [12].

The power spectra corresponding to the time traces in Figs. 2(a) and 2(c) are shown in Fig. 3 as grey and black curves, respectively. Only the CCW spectra are shown as they are nearly identical to the CW spectra. In Fig. 3(i), the spectra are shown in a baseband frequency range. The spectra possess the SW fundamental frequency at $T^{-1} \approx 10.5$ MHz and consist of only the odd harmonics as the SWs are symmetric. As η increases from -36 dB to -27 dB, an enhancement of the high-order harmonics is observed together with a reduction of electrical linewidths, which is due to the reduction of the switching time τ_s. The details of the normalized fundamental frequency components are shown with respect to the frequency offset from T^{-1} in Fig. 3(ii). At the weak feedback of $\eta = -36$ dB, the spectrum is relatively broad with a 3-dB linewidth of $\Delta f = 670$ kHz (grey trace). As the feedback strengthens to $\eta = -27$ dB, the spectrum is significantly narrowed to $\Delta f = 1.1$ kHz (black trace), which corresponds to an improvement of the temporal regularity of the SW [12, 16]. For completeness, Fig. 4 shows the optical spectra of the SRL with the CCW and CW emission shown in black and red, respectively. In Fig. 4(a), the SRL is free-running without any feedback so that there is only CCW emission according to Fig. 1(b). The optical spectrum shows a single-mode operation with a side-mode suppression ratio approaching 30 dB [7]. When the SRL is subject to feedback and exhibits SW oscillations, the CCW and CW optical spectra become multi-moded as shown in Fig. 4(b).

For the SW intensity oscillations, the switching time τ_s and the electrical linewidth Δf are characterized in more detail as a function of the feedback efficiency and laser bias in Figs. 5(a) and 5(b), respectively. The switching time is averaged over many SW cycles and the linewidth is measured around the fundamental frequency on the RF spectrum analyser. The closed symbols in Fig. 5 show measurement data in which the feedback efficiency η is varied while the SRL bias current is kept at a constant value of $I = 260$ mA. At $\eta = -36$ dB, the weak feedback is merely sufficient to drive the SRL from continuous-wave operation into regular periodic SW switching. This results in a relatively large switching time $\tau_s = 4.5$ ns and a relatively broad electrical linewidth $\Delta f = 670$ kHz, which correspond to the time traces in Fig. 2(a) and to the grey spectrum in Fig. 3. As η increases, the feedback is reinforced so that both the switching time τ_s and the electrical linewidth gradually reduce. It can also be observed that for η greater than approximately -27 dB, τ_s and Δf do not reduce any longer. The minimum switching time is on the order of 1 ns, which is comparable to the recovery time in SRLs subject to external injection and to modal switching triggered by backscattering [6, 7, 12]. For instance, alternate oscillations due to intra-cavity backscattering that couples CCW and CW lasing modes as well as relaxation oscillations due to pulsation of charge carriers have been reported on a similar time scales [6, 7]. Moreover, it is worth noting in Fig. 5 that SRLs with feedback can be driven to chaotic dynamics if a larger η beyond -24 dB is adopted [24, 25]. The open symbols in Fig. 5 show data in which the SRL bias current I is varied while η is kept at a constant value of -27 dB. No significant variations in τ_s and Δf are observed for a bias ranging from 200 mA to 275 mA, which covers a few switchings of the free-running lasing direction as shown in Fig. 1(b).

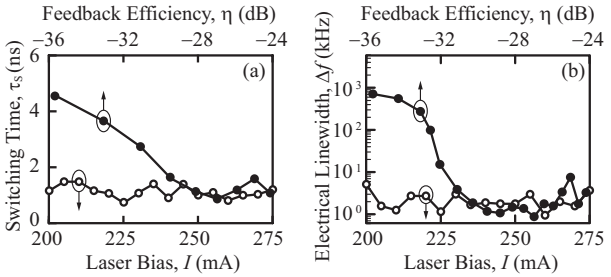

Fig. 5. (a) Switching time τ_s and (b) electrical linewidth Δf of the SW output intensities from the SRL subject to feedback with $\tau_1 = \tau_2 = 45$ ns. Both η and I are varied.

In lieu of equal delays, Fig. 6 shows the intensity-time traces obtained using unequal delays. Keeping τ_1 fixed at 45 ns, different values of τ_2 are used. In the measurements of Figs. 6(a)–6(c), η is kept at a fixed value of -36 dB, τ_2 is set at 66 ns, 108 ns, and 163 ns, respectively. For each case, the SRL emits in the CCW direction for a duration of τ_1 and then switches to the CW direction for a duration of τ_2, which is followed by switching back to the CCW direction. Therefore, asymmetric SWs are obtained with a duty cycle of $\tau_1/(\tau_1 + \tau_2)$. Such asymmetric SWs with tunability of the duty cycle cannot be achieved using the one-way feedback previously reported [12, 16]. The outputs in CCW (black) and CW (red) are again complementary, where the period T is approximately $\tau_1 + \tau_2$.

Interestingly, high-order symmetric SWs with period $T = (\tau_1 + \tau_2)/n$ are also solutions to the mutual feedback geometry, where n is an integral order. Such high-order SWs are possible when $\tau_{1,2}$ are odd multiples of $T/2$ [14]. For Figs. 6(d)–6(f), τ_2 is respectively set at 108 ns, 190 ns, and 93 ns, where η is optimized at values between -24 dB and -20 dB for exciting the solution with high-order SWs. Only the CCW outputs are shown for clarity. In Fig. 6(d), the SW has $T = 31$ ns which is approximately $2\tau_1/3 \approx (\tau_1 + \tau_2)/5$. In Fig. 6(e), the SW has $T = 19$ ns which is approximately $2\tau_1/5 \approx (\tau_1 + \tau_2)/12$.

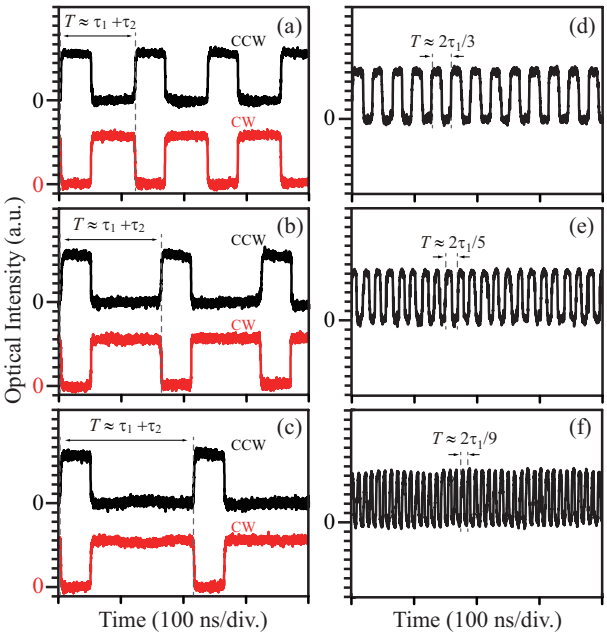

Fig. 6. Intensity-time traces of the SRL subject to feedback with τ_1 = 45 ns and (a) τ_2 = 66 ns, (b) τ_2 = 108 ns, and (c) τ_2 = 163 ns at $\eta = -36$ dB. High-order SWs are obtained when τ_2 is (d) 108 ns, (e) 190 ns, and (f) 93 ns at optimal η.

Finally, in Fig. 6(f), the SW has T = 10.3 ns which is approximately $2\tau_1/9 \approx (\tau_1 + \tau_2)/13$, corresponding to a high order of $n = 13$. For constant $\tau_{1,2}$, the order n generally increases when the feedback efficiency increases. A similar observation has been reported in a laser with polarization-rotated feedback as the delay was varied [14]. The excitation of the high-order symmetric SWs yields short periods that circumvent the practical difficulties in realizing short delay paths. This higher order SW solution is currently being explored in more detail so as to gather a full understanding of the phenomenon.

In summary, a SRL subject to mutual feedback is experimentally investigated by feeding back the CCW emission into the CW direction after a duration of τ_1, and the CW emission into the CCW direction after a duration of τ_2. The lasing direction is observed to switch periodically at $T \approx \tau_1 + \tau_2$, resulting in complementary SWs in the emission intensities in the CCW and CW directions. Symmetric SWs are observed when $\tau_1 = \tau_2$, where both the switching time τ_s and the electrical linewidth Δf reduce as the feedback strengthens. Minimal values of τ_s=1.4 ns and Δf = 1.1 kHz were observed experimentally. Asymmetric SWs are observed when $\tau_1 \neq \tau_2$, where the duty cycle is about $\tau_1/(\tau_1 + \tau_2)$. High-order SWs are also observed at specific combinations of τ_1 and τ_2, where the period is reduced to $T = (\tau_1 + \tau_2)/n$. We experimentally demonstrated a high-order solution with a period of T = 10.3 ns and n as high as 13. The SRL geometry will allow in the future to directly integrate short feedback paths on the bus waveguides so as to reduce the period further and to make the whole geometry very compact.

This work was supported by the Royal Society under Project IE120157 and the Research Grants Council of Hong Kong under Projects CityU 110712 and CityU 11201014. The authors acknowledge the staff at the James Watt Nanofabrication Centre at Glasgow University.

REFERENCES

1. M. Sorel, P. J. R. Laybourn, G. Giuliani, and S. Donati, Appl. Phys. Lett. **80**, 3051 (2002).
2. H. Zeghlache, P. Mandel, N. B. Abraham, L. M. Hoffer, G. L. Lippi, and T. Mello, Phys. Rev. A **37**, 470 (1988).
3. S. Beri, L. Gelens, M. Mestre, G. Van der Sande, G. Verschaffelt, A. Scire, G. Mezosi, M. Sorel, and J. Danckaert, Phys. Rev. Lett. **101**, 093903 (2008).
4. X. Cai, Y. L. D. Ho, G. Mezosi, Z. Wang, M. Sorel, and S. Yu, IEEE J. Quantum Electron. **48**, 406 (2012).
5. J. Javaloyes and S. Balle, IEEE J. Quantum Electron. **45**, 431 (2009).
6. M. Sorel, G. Giuliani, A. Scire, R. Miglierina, S. Donati, and P. J. R. Laybourn, IEEE J. Quantum Electron. **39**, 1187 (2003).
7. A. Trita, G. Mezosi, M. J. Latorre-Vidal, M. Zanola, M. J. Strain, F. Bragheri, M. Sorel, and G. Giuliani, IEEE J. Quantum Electron. **49**, 877 (2013).
8. A. Trita, G. Mezosi, M. Sorel, and G. Giuliani, IEEE Photon. Technol. Lett. **26**, 96 (2014).
9. J. Javaloyes and S. Balle, IEEE J. Quantum Electron. **47**, 1078 (2011).
10. T. Perez, A. Scire, G. Van der Sande, P. Colet, and C. R. Mirasso, Opt. Express **15**, 12941 (2007).
11. B. Li, M. I. Memon, G. Mezosi, Z. Wang, M. Sorel, and S. Yu, J. Lightwave Technol. **27**, 4233 (2009).
12. L. Mashal, G. Van der Sande, L. Gelens, J. Danckaert, and G. Verschaffelt, Opt. Express **20**, 22503 (2012).
13. A. Gavrielides, T. Erneux, D. W. Sukow, G. Burner, T. McLachlan, J. Miller, and J. Amonette, Opt. Lett. **31**, 2006 (2006).
14. G. Friart, G. Verschaffelt, J. Danckaert, and T. Erneux, Opt. Lett. **39**, 6098 (2014).
15. G. Friart, L. Weicker, J. Danckaert, and T. Erneux, Opt. Express **22**, 690 (2014).
16. J. Mulet, M. Giudici, J. Javaloyes, and S. Balle, Phys. Rev. A **76**, 043801 (2007).
17. D. W. Sukow, T. Gilfillan, B. Pope, M. S. Torre, A. Gavrielides, and C. Masoller, Phys. Rev. A **86**, 033818 (2012).
18. M. Marconi, J. Javaloyes, S. Barland, M. Giudici, and S. Balle, Phys. Rev. A **87**, 013827 (2013).
19. A. M. Kaplan, G. P. Agrawal, and D. N. Maywar, IEEE Photon. Technol. Lett. **22**, 489 (2010).
20. L. Weicker, T. Erneux, O. D'Huys, J. Danckaert, M. Jacquot, Y. Chembo, and L. Larger, Phys. Rev. E **86**, 055201 (2012).
21. X. Zhang, C. Gu, G. Chen, B. Sun, L. Xu, A. Wang, and H. Ming, Opt. Lett. **37**, 1334 (2012).
22. M. Peil, M. Jacquot, Y. K. Chembo, L. Larger, and T. Erneux, Phys. Rev. E **79**, 026208 (2009).
23. D. W. Sukow, A. Gavrielides, T. Erneux, B. Mooneyham, K. Lee, J. McKay, and J. Davis, Phys. Rev. E **81**, 025206 (2010).
24. I. V. Ermakov, G. Van der Sande, and J. Danckaert, Commun. Nonlinear Sci. Numer. Simul. **17**, 4767 (2012).
25. R. M. Nguimdo, G. Verschaffelt, J. Danckaert, and G. Van der Sande, Opt. Lett. **37**, 2541 (2012).